Hydroxycarboxylic acid receptor 3 and GPR84 – two metabolite-sensing G protein-coupled receptors with opposing functions in innate immune cells

Anna Peters[1], Philipp Rabe[1], Aenne-Dorothea Liebing[1], Petra Krumbholz[1], Anders Nordström[2], Elisabeth Jäger[3], Robert Kraft[4], Claudia Stäubert[1]*

[1] Rudolf Schönheimer Institute of Biochemistry, Faculty of Medicine, Leipzig University, Johannisallee 30, 04103 Leipzig, Germany

[2] Swedish Metabolomics Centre, Department of Forest Genetics and Plant Physiology, Swedish University of Agricultural Sciences, Linnaeus väg 6, 901 87 Umeå, Sweden

[3] Cedars-Sinai Medical Center, Department of Pathology, 8700 Beverly Blvd, 90048 Los Angeles (CA), USA

[4] Carl Ludwig Institute for Physiology, Faculty of Medicine, Leipzig University, Liebigstraße 27, 04103 Leipzig, Germany

* To whom correspondence and requests for materials should be addressed:
Claudia Stäubert, Rudolf Schönheimer Institute of Biochemistry, Faculty of Medicine, Leipzig University, Johannisallee 30, 04103 Leipzig, Germany, Tel.: +49-341-9722-157, Fax: +49-341-9722-159, Email: claudia.staeubert@medizin.uni-leipzig.de

The data that support the findings of this study are provided with the manuscript and the supplementary material.

AP acquired, analyzed and interpreted data (DMR, cAMP, ERK, AKT, IP_1, TNFα, NFκB seahorse, image-based analyses) and drafted the manuscript. ADL carried out experiments and analyzed data (cAMP, ERK, AKT, ROS). PR carried out and analyzed the RT-qPCR experiments. PK carried out experiments (cAMP, ERK, AKT). AN carried out the LC-MS experiments. RK performed the Ca^{2+} imaging experiments, analyzed and visualized this data. EJ performed the IL-1β experiments. CS performed the *E. coli* growth curve and analyzed the LC-MS experiments. CS analyzed, interpreted and visualized the data, conceptually and experimentally designed the work, supervised the study and wrote the manuscript. All authors discussed the results, their implications and commented on the manuscript at all stages. All authors read and approved the final manuscript.

The authors declare that no competing interests exist.

The studies with human materials were conducted in accordance with the Declaration of Helsinki and with the recommendations of "Ethik-Kommission an der Medizinischen Fakultät der Universität Leipzig" with written informed consent from all blood donors. The protocol was approved by the aforementioned committee (313/14-ek).

Running Title: Reciprocal modulation of innate immunity by HCA_3 and GPR84

Abstract

G protein-coupled receptors (GPCRs) are key regulatory proteins of immune cell function inducing signaling in response to extracellular (pathogenic) stimuli. Although unrelated, hydroxycarboxylic acid receptor 3 (HCA_3) and GPR84 share signaling via $G\alpha_{i/o}$ proteins and the agonist 3-hydroxydecanoic acid (3HDec). Both receptors are abundantly expressed in monocytes, macrophages and neutrophils but have opposing functions in these innate immune cells. Detailed insights into the molecular mechanisms and signaling components involved in immune cell regulation by GPR84 and HCA_3 are still lacking.

Here, we report that GPR84-mediated pro-inflammatory signaling depends on coupling to the hematopoietic cell-specific $G\alpha_{15}$ protein in human macrophages, while HCA_3 exclusively couples to $G\alpha_i$ protein. We show that activated GPR84 induces $G\alpha_{15}$-dependent ERK activation, increases intracellular Ca^{2+} and IP_3 levels as well as ROS production. In contrast, HCA_3 activation shifts macrophage metabolism to a less glycolytic phenotype, which is associated with anti-inflammatory responses. This is supported by an increased release of anti-inflammatory IL-10 and a decreased secretion of pro-inflammatory IL-1β. In primary human neutrophils, stimulation with HCA_3 agonists counteracts the GPR84-induced neutrophil activation. Our analyses reveal that 3HDec acts solely through GPR84 but not HCA_3 activation in macrophages.

In summary, this study shows that HCA_3 mediates hyporesponsiveness in response to metabolites derived from dietary lactic acid bacteria and uncovers that GPR84, which is already targeted in clinical trials, promotes pro-inflammatory signaling via $G\alpha_{15}$ protein in macrophages.

Keywords

hydroxycarboxylic acid receptor 3; GPR84; macrophages; neutrophils; D-phenyllactic acid; Lactic acid bacteria

Chemical compounds studied in this article

3-Hydroxydecanoic acid (PubChem CID: 26612); 3-Hydroxyoctanoic acid (PubChem CID: 26613); D-(+)-3-Phenyllactic acid (PubChem CID: 643327); 1-(1-Methylethyl)-1H-benzotriazole-5-carboxylic acid (PubChem CID: 2736690); Decanoic acid (PubChem CID: 2969); 6-n-Octylaminouracil (PubChem CID: 10354234)

Abbreviations:

3HDec, 3-hydroxydecanoic acid; 3HO, 3-hydroxyoctanoic acid; AC, adenylyl cyclase; C10, decanoic acid; cAMP, cyclic adenosine monophosphate; DHR123, dihydrorhodamine 123; DMR, dynamic mass redistribution; DPI, diphenyleneiodonium chloride; D-PLA, D-phenyllactic acid; ECAR, extracellular acidification rate; ETC, electron transport chain; fMLP, N-formylmethionyl-leucyl-phenylalanine; GPCR, G protein-coupled receptor; HCA, hydroxycarboxylic acid receptor; IL, interleukin; IP_1, inositol monophosphate; IPBT-5CA, 1-(1-Methylethyl)-1H-benzotriazole-5-carboxylic acid; LAB, lactic acid bacteria; LPS, lipopolysaccharides; MCFA, medium-chain fatty acid; NFκB, nuclear factor κ B; NET, neutrophil extracellular traps; NOX, NADPH oxidase; OCR, oxygen consumption rate; PI, propidium iodide; PLC, phospholipase C; PMA, phorbol 12-myristate 13-acetate; PMNs, polymorphonuclear neutrophil leucocytes; PTX, pertussis toxin; ROS, reactive oxygen species; TNFα, tumor necrosis factor α

1. Introduction

Hydroxycarboxylic acid receptor 3 (HCA_3) and GPR84 are both rhodopsin-like G protein-coupled receptors (GPCRs). GPR84 has first been deorphanized as a receptor for medium-chain fatty acids (MCFAs) (C10 – C14) and their 3-hydroxy derivatives, while HCA_3 was initially shown to be activated by the fatty acid oxidation intermediate 3-hydroxyoctanoic acid (3HO) [1,2]. Although GPR84 and HCA_3 are rather distantly related, both receptors have in common that they are abundantly expressed in innate immune cells, coupled to $G\alpha_{i/o}$ proteins, and activated by 3-hydroxydecanoic acid (3HDec) [1,3,4]. Despite these shared features, we recently showed differential signaling outcome of HCA_3 and GPR84 in response to 3HDec [5]. Our observations from a heterologous expression system suggested that differences in endocytosis and signaling upon activation of GPR84 and HCA_3 may result in distinct physiological responses in cells endogenously expressing the receptors, like e.g. macrophages and neutrophils [5]. In immune cells, GPR84 has been associated with pro-inflammatory responses including induction of chemotaxis, phagocytosis and enhanced cytokine release [6–8]. For HCA_3, we recently showed that fermented food-derived metabolites of lactic acid bacteria (LAB), such as D-phenyllactic acid (D-PLA), are highly potent agonists [3]. Many studies demonstrate that D-PLA increases immune tolerance through activation of anti-inflammatory processes (summarized in [3]) thus suggesting that HCA_3 mediates some of these effects. There are only a few studies on the physiological function of HCA_3 since it is only present in humans and great apes and therefore accessible animal models are lacking [3,9] .

Our present study is based on the assumption that the specific effects of different agonists acting on HCA_3 and GPR84 are the basis for recognizing their function in immune cells. Since the bacterial origin of 3HDec, which activates both receptors, has only been shown indirectly in clinical samples [10], we analyzed *in vitro E. coli* culture medium for their relative 3HDec concentration in different growth phases. Further, we aimed to elucidate the molecular mechanisms relevant for the interplay of HCA_3 and GPR84 in innate immune cells. Macrophages polarized from the human monocytic THP-1 cell line and freshly isolated polymorphonuclear neutrophil leucocytes (PMNs) were analyzed regarding their HCA_3 and GPR84-mediated cellular functions. Both, macrophages and PMNs provide the first line of defense against invading microorganisms [11,12] and their cellular functions include phagocytosis, chemotaxis, the production of reactive oxygen species (ROS) as well as the release of anti-microbial peptides, lytic enzymes and different cytokines [13–15].

We found that although both, HCA_3 and GPR84, are described as solely coupled to $G\alpha_{i/o}$, GPR84 is also coupled to the $G\alpha_{15}$ protein in macrophages. Activation of GPR84 by C10 and 3HDec caused a $G\alpha_{15}$ protein-mediated increase in intracellular Ca^{2+} levels, IP_1 levels and ERK activation, associated with an enhanced ROS production. In contrast to our own previously obtained data in heterologous expression systems [5], here no HCA_3-mediated effects upon activation by 3HDec were observed. However, stimulation of HCA_3 by D-PLA, 3HO or the surrogate agonist IPBT-5CA reduced interleukin-1β (IL-1β) secretion, but increased anti-inflammatory interleukin-10 secretion in macrophages. This is reflected metabolically by a less glycolytic phenotype in presence of HCA_3 agonists, which is a characteristic feature of anti-inflammatory responses of macrophages [16]. Similarly, we show that GPR84 agonists activate PMNs, while this is counteracted by HCA_3 signaling.

2. Materials and Methods

2.1 Chemicals and Media

All compounds, inhibitors and cytokines were purchased from Sigma-Aldrich, Cayman Chemical or Santa Cruz Biotechnology if not stated otherwise. All protocols were followed according to the respective manufacturers' instructions, if not explicitly specified differently.

All media, antibiotics and fetal bovine serum (FBS) were obtained from Thermo Fisher Scientific if not stated otherwise. HBSS buffer was supplemented with 20 mM HEPES and the pH was adjusted to 7.4 if not stated otherwise.

2.2 Isolation of PMNs (polymorphonuclear neutrophil leucocytes)

Blood was taken from healthy blood donors and experiments were conducted in accordance with the Declaration of Helsinki according to a protocol approved by the Ethics Review Board of the Medical Faculty, Leipzig University (313/14-ek and 430/16-ek), with written informed consent from all blood donors.

PMNs were freshly isolated from human peripheral blood employing the alternate protocol described by Kuhns et al. [17]. In brief, following Ficoll-Paque-based density gradient centrifugation, the PMN- and erythrocyte-rich pellet was mixed with 3 % dextran to separate them by allowing the erythrocytes to sediment at 1 x g for 20 min. Subsequently, the PMN-rich supernatant was centrifuged at 300 x g for 10 min, remaining erythrocytes in the PMN-containing pellet were lysed (2 cycles), finally cells were washed, resuspended in HBSS (-) (without Calcium/Magnesium) and stored at RT at a density of 1 - 2.5 x 10^7 cells/ml until seeded for respective assay. If not otherwise stated, for all analyses involving PMNs, 5 x 10^4 freshly isolated cells per well were seeded in a 96-well plate in HBSS.

2.3 Cell culture

THP-1 cells obtained from the DSMZ-German Collection of Microorganisms and Cell Cultures, THP-1-Lucia NFκB cells, stably expressing an NFκB-inducible Lucia reporter construct, purchased from InvivoGen and the human embryonic kidney cell line HEK293-T (ATCC CRL-3216) were maintained at 37 °C in a humidified 5 % CO_2 incubator. Both THP-1 cell lines were grown in RPMI-1640 supplemented with 10 % heat inactivated (HI, 30 min at 56 °C) fetal bovine serum (FBS), 100 U/ml penicillin and 100 µg/ml streptomycin and split every 3-4 days (THP-1 cells: 4 x 10^6 cells/T75-flask in 20 ml, THP-1-LuciaNFκB cells: 10 x 10^6 cells/T75-flask in 20 ml). Medium of THP-1-Lucia NFκB was additionally supplemented with 100 µg/ml Normocin (InvivoGen) and every other passage with 100 µg/ml Zeocin. Activation of the NFκB-inducible Lucia reporter results in secretion of luciferase into the cell culture supernatant. HEK293-T cells were cultured in Dulbecco's Modified Eagle medium (DMEM) containing 10 % FBS, 100 U/ml penicillin and 100 µg/ml streptomycin.

2.3.1 Differentiation and polarization of THP-1 cells

THP-1 cells were split into 96-well (analyses-dependent: Greiner or Seahorse XF cell culture plates) or 24-well plates (depending on the assay) at a density of 5 x 10^4 or 5 x 10^5 cells/well and differentiated with 50 ng/ml PMA for 48 h. To subsequently polarize THP-1 cells into M0-, M1- or M2-like macrophages, cells were incubated for another 48 h in RPMI-1640 supplemented with 10 % HI- FBS (M0), RPMI-1640 + 10 % HI-FBS + 20 ng/ml LPS + 20 ng/ml IFNγ (M1), or RPMI-1640 + 10 % HI-FBS + 25 ng/ml IL-4 + 25 ng/ml IL-13 (M2) as previously described [18]. THP-1-Lucia NFκB cells were differentiated and polarized using the same protocol, only the cell density was adapted to 1 x 10^5 cells/well in 96-well plates.

THP-1 cells were polarized to M1-like macrophages for RT-qPCR analyses, cAMP inhibition and IP_1 accumulation assays, ERK and AKT activation analyses, detection of human IL-1β and TNFα, prior Ca^{2+} imaging and analyses of ROS production as well as for the Seahorse XF Cell Mito Stress Test.

2.3.2 siRNA transfection of THP-1 cells

Differentiated THP-1 cells were transfected with siRNA (OriGene) specifically targeting HCA_3, GPR84 or GNA15 (supplementary Table S1), respectively, using Viromer Green (Lipocalyx). Prior to the transfection, the medium was changed to M1-polarizing medium. 10

µl or 100 µl of siRNA-Viromer mix were added to each well in 96- or 24-well plates, respectively. Assays were performed 24 h - 48 h post transfection.

2.4 RNA preparation, reverse transcription and quantitative real-time PCR

For preparation of RNA the ReliaPrep RNA Cell Miniprep System (Promega) was used. RNA of freshly isolated PMNs (1.7 x 10^6 ≈ PMNs in 1 ml blood) was extracted using the SV Total RNA Isolation System (Promega). PMNs were centrifuged and immediately lysed in lysis buffer supplied with the Kit. THP-1 cells were seeded in 24-well plates (5 x 10^5 cells/well), differentiated and polarized to M0-, M1- or M2-like macrophages and then harvested. Yielded RNA concentrations were measured using a Nano Drop spectrophotometer and RNA was stored at -80 °C.

Prior to reverse transcription, 500 ng RNA were treated with 1 µl DnaseI (NEB) in a total reaction volume of 10 µl for 30 min at 37 °C. Reactions were stopped by addition of 1 µl 50 mM EDTA and heat inactivation for 10 min at 75 °C. Directly thereafter, RNA was reverse transcribed using iScript cDNA Synthesis Kit (Bio-Rad). Transcribed cDNA was diluted with RNase-free H_2O to a final volume of 70 µl. The qPCR set-up was as follows: each reaction (12 µl) contained 1 µl of cDNA, 1 µl of premixed sense and anti-sense primer (400 nM each), 5 µl of RNase-free H_2O and 5 µl of Luna Universal qPCR Master Mix (NEB).

The following thermal cycling protocol was used: polymerase activation at 95 °C for 2 min, followed by 40 cycles of 15 s of denaturation at 95 °C and 30 s of monitored annealing/extension at 60 °C. Subsequently, melt curves were recorded (55 °C – 95 °C, 0.5 °C increment, 5 s/step). Real-time PCR and data collection (C_q determination mode: regression) were performed on Bio-Rad CFX Connect Real-Time PCR Detection System. Indicated n reflect biological replicates, that were reverse-transcribed and qPCR was run in duplicates. Primers were designed using Primer-Blast (http://www.ncbi.nlm.nih.gov/tools/primer-blast/) and ordered from Microsynth Seqlab. Melt curves after the qPCR run showed one single sharp peak for each primer pair listed in supplementary Table S1.

2.5 Functional assays

2.5.1 Dynamic mass redistribution (DMR) assay

To measure label-free receptor activation, DMR Measurements (Epic technology, Corning Life Sciences) were performed with PMNs. Freshly isolated PMNs were resuspended in HBSS with or without 3 µg/ml PTX and incubated for 60 min at RT prior to seeding them in an uncoated Epic 384-well microplate at a density of 8 x 10^4cells per well. Seeding was followed by 45 min of equilibration, subsequent stimulation with various agonists was performed and DMR was recorded for 60 min. In DMR measurements, polarized light is passed through the bottom of the biosensor microplate, and a shift in wavelength of reflected light indicates intracellular mass redistribution triggered by receptor activation.

2.5.2 ALPHAScreen cAMP assay

Cyclic AMP content of cell extracts was determined using the ALPHAScreen cAMP Detection Kit (Perkin Elmer). Stimulation with various agonists at different concentrations was performed in HBSS with 1 mM 3-isobutyl-1-methylxanthine (IBMX) and 2 µM forskolin for 15 min at 37 °C. Reactions were stopped by aspiration of stimulation buffer and cells were lysed in 100 µl/well of lysis buffer containing 1 mM IBMX. From each well 5 µl of lysate were transferred to a 384-well plate and proceeded as previously described [5].

2.5.3 Alpha SureFire Multiplex pERK 1/2 & total ERK Assay and pAKT1/2/3 & total AKT1 Assay

The pERK/total ERK and pAKT/total AKT ratios of cell extracts were determined using the Alpha SureFire Ultra Multiplex p-ERK 1/2 (Thr202/Tyr204) & Total ERK assay and the p-AKT1/2/3(Ser473) & Total AKT1 assay technology, respectively (Perkin Elmer).

For both assays, THP-1 cells and freshly isolated PMNs were seeded in 96-well plates. Stimulation with agonists was performed in HBSS buffer with 20 mM HEPES for 10 min at 37 °C. For assays with both cell types, reactions were stopped by aspiration of stimulation buffer and lysis of cells in 50 µl/well of supplied lysis buffer supplemented with 250 µM protease inhibitor cocktail Pefabloc (AEBSF). From each well 10 µl of lysate were transferred to a 384-well plate and acceptor beads and donor beads were added.

2.5.4 HTRF IP_1 assay

IP_1 content of cell extracts was determined by using the HTRF Technology (Cisbio). Stimulation with various agonists at different concentrations was performed in 35 µl/well supplied stimulation buffer for 60 min at 37 °C. Reactions were stopped by placing cells on ice and addition of 30 µl/well of supplied lysis buffer. From each well 7 µl of lysate were transferred to a 384-well low volume plate. Acceptor and donor antibodies were added.

2.5.5 Ca^{2+} imaging

THP-1 cells, polarized to M1-like macrophages and transfected with siRNA when applicable, were seeded in 24-well plates on glass cover slips. For imaging experiments, cells were loaded with 5 µM fura-2AM (Molecular Probes) for 60 min in a standard solution containing 140 mM NaCl, 10 mM HEPES, 5 mM KCl, 2 mM $CaCl_2$, 1 mM $MgCl_2$, and 10 mM glucose. Fura 2-based measurements were performed in single cells using a monochromator-based imaging system and the software TILLvisION 4.0 (T.I.L.L. Photonics). Emitted fluorescences (excited at 340 nm and 380 nm) were acquired with a CCD camera (PCO Imaging) at intervals of 2 s and corrected for background fluorescence. Stock solutions of GPR84 and HCA_3 agonists as well as fMLP and ATP were dissolved in standard solution and applied to the cells by bath perfusion.

2.5.6 Detection of Human IL-1β, IL-10, TNFα

Human IL-1β, IL-10 and TNFα concentrations in cell culture supernatants were determined employing the Human IL-1β ELISA Set II (BD Bioscience), the Human IL-10 ELISA Set (BD Bioscience) and the Human TNFα HTRF-Kit (Cisbio), respectively, according to the manufacturer's protocol. Stimulation with agonists was performed in RPMI-1640 + 10 % FBS 37 °C (8 h, 500 µl/well: IL-1β, IL-10; 5 h, 60 µl/well: TNFα). Reactions were stopped by aspiration of supernatants, which were subsequently frozen and stored (IL-1β, IL-10: -20 °C, TNFα: -80 °C) for later analysis.

2.5.7 NFκB luciferase assay

THP-1-Lucia NFκB cells were seeded in 96-well plates and differentiated with PMA for 48 h. Stimulation with agonists was performed in M1-polarization medium (using RPMI-1640 without phenol red) for 48 h at 37 °C and 5 % CO_2. To measure luciferase activity corresponding to NFκB activation, 20 µl/well of cell culture supernatant were transferred to a black 96-well plate, 50 µl/well of QUANTI-Luc assay solution (InvivoGen,) were added in the dark and luminescence was immediately measured using the EnVision multimode plate reader (Perkin Elmer).

2.5.8 Seahorse XF Cell Mito Stress Test

THP-1 cells were seeded in 96-well Seahorse XF cell culture plates and polarized to M1-like macrophages. Medium was changed to Phenol Red-free non-buffered Seahorse XF RPMI Medium containing 10 mM glucose, 2 mM L-glutamine, and 1 mM sodium pyruvate. The oxygen consumption rate (OCR) and extracellular acidification rate (ECAR) were measured using the mitochondrial stress test (Agilent) according to the manufacturer's protocol under basal conditions and in response to 1 µM oligomycin, 0.5 µM fluoro-carbonyl cyanide phenylhydrazone (FCCP) and 0.5 µM rotenone / 0.5 µM antimycin A with the XF96 Extracellular Flux Analyzer (Seahorse Bioscience). ECAR, a proxy for lactate production, and OCR were recorded to assess the glycolytic activity and mitochondrial respiratory activity, respectively. Upon completion of the Seahorse assay, cells were stained with Hoechst 33342

(1:5000, Sigma-Aldrich) for 15 min at 37 °C to determine the total cell numbers per well. Plates were imaged and automatically analyzed using the Celigo Imaging Cytometer (Nexcelom Bioscience). Cell count was used for normalization of Seahorse Mito Stress Test data. The components of the ETC are localized in mitochondria and composed of complex I (inhibited by rotenone), complex II, complex III (inhibited by antimycin A), and complex IV, which reduces oxygen (OCR) (Figure 4C). The proton gradient generated by electron transfer along the ETC is used by the ATP synthase (inhibited by oligomycin) to generate adenosine triphosphate (ATP). FCCP uncouples the ETC from ATP production by depletion of the proton gradient. The ECAR reflects the cytosolic proton concentration, which is a measure of the rate of glycolysis. The parameters were calculated as follows: ***non-mitochondrial oxygen consumption*** (= minimum rate OCR measurement after rotenone / antimycin A injection), ***basal respiration*** (baseline OCR - non-mitochondrial respiration), ***ATP production*** (basal respiration - OCR after oligomycin injection), ***maximal respiration*** (maximum OCR after FCCP injection - non-mitochondrial respiration), ***spare respiratory capacity as %*** (maximal respiration / basal respiration x 100).

2.5.9 Determination of HCA_3 and GPR84 knockdown efficiency using ELISA

HEK-293T cells were seeded in T-25 cell culture flasks (1.6 x 10^6 cells/flask) and co-transfected with receptor-specific siRNA or siNC and plasmid encoding N-terminally HA-tagged GPR84 or N-terminally HA-tagged HCA_3, respectively. Plasmids described in [5]. Lipofectamine 2000 (Life Technologies, Darmstadt, Germany) with 2 µg plasmid and 200 pmol siRNA was used for transient transfection. 24 h after transfection, cells were harvested and plated in 48-well plates (1 x 10^5 cells/well; cell surface expression). Cell surface expression was measured using an direct cellular ELISA as described in [5].

2.6 Image-based analyses

2.6.1 ROS formation

To measure NADPH oxidase-dependent ROS formation, THP-1 cells were seeded in 96-well plates, incubated with 5 µM dihydrorhodamine 123 (DHR123), and stimulated with receptor agonists for 24 h at 37 °C in the presence or absence of 4 µM NADPH oxidase inhibitor diphenyleneiodonium chloride (DPI). The assay was performed in HBSS containing 10 % THP-1 cell culture medium. Following incubation, buffer containing agonists and DHR123 +/- DPI was removed from plates and replaced by fresh HBSS. Plates were imaged immediately and automatically analyzed using the Celigo Imaging Cytometer (Nexcelom Bioscience).

2.6.2 PMN activation/NET formation assay

PMNs were seeded in 96-well plates, receptor agonists were added, followed by incubation at 37 °C for 20 h. Finally, PMNs were stained with propidium iodide (PI, 1:2500, 1 mg/ml stock, Thermo Fisher Scientific) and Hoechst 33342 (1:5000, Sigma-Aldrich) for 15 min at 37 °C to measure activated and total cell numbers, respectively. Plates were imaged and automatically analyzed using the Celigo Imaging Cytometer (Nexcelom Bioscience).

2.6.3 Phagocytosis

PMNs were seeded in black Greiner 96-well plates with clear bottom, receptor agonists were added, followed by incubation at 37 °C for 30 min. The *E. coli* pHrodo Red-conjugated BioParticles (Thermo Fisher Scientific) were added to the plate at a final concentration of 0.1 mg/ml, followed by incubation at 37 °C for 60 min. Subsequently, the *E. coli* particles were removed, cells were washed 3 x with PBS and fixed with 4 % formalin for 15 min at room temperature (RT). Next, the cells were washed once with PBS, permeabilized using 0,5 % Triton X-100 in PBS at RT for 10 min, washed twice with PBS and finally stained with Alexa Fluor 488 Phalloidin (1:40, Thermo Fisher Scientific) and Hoechst 33342 (1:5000) for 10 min at RT. Plates were imaged and analyzed using the Celigo Imaging Cytometer (Nexcelom

Bioscience). Confocal images were acquired using a 40 x objective employing the Confocal Quantitative Image Cytometer CQ1 (Yokogawa/Cenibra).

2.7 Liquid Chromatography Mass Spectrometry (LC-MS) measurement

E. coli K-12 MG1655 were cultured for 24 hours in M9 mineral medium containing M9 salt solution (33.7 mM Na_2HPO_4, 22 mM KH_2PO_4, 8.55 mM NaCl, 9.35 mM NH_4Cl) supplemented with 20 µM uracil, 60 µM threonine, 60 µM leucine, 20 µM histidine, 22 µM glucose, 2 mM $MgSO_4$, and 100 µM $CaCl_2$. OD_{600} was determined every 30 min for 8 h and again 24 h after the start of the experiment. Samples corresponding to ~ 20 mg *E. coli* wet weight were taken at OD_{600} 0.2 (50 ml), 0.4 (15 ml), 0.7 (10 ml) and at time point 24 h (4 ml) and centrifuged (2000 x g) at 4°C for 10 min. Of the resulting supernatant 250 µl were directly added to an Eppendorf tube containing 750 µl ice-cold MeOH. Tubes were incubated 20 min at -20°C, centrifuged (14.000 rpm) for 10 min at 4°C and 400 µl of supernatant were transferred to LC-MS glass vials, dried down in a speed vacuum concentrator and stored at -20°C until analysis. Samples were dissolved in 20 µl 50:50 MeOH:H_2O of which 2 µl were injected into the Agilent 1290 LC-system connected to a 6550 Agilent Q-TOF mass spectrometer and an electrospray ionization (ESI) source was used. Data was collected in negative ionization mode. ESI (Agilent Jetstream) settings were as follows; gas temperature 300°C, gas flow 8 l/min, nebulizer pressure 40 psi, sheet gas temperature 350°C, sheet gas flow 11, Vcap 4000, fragmentor 100, Skimmer1 45 and OctapoleRFPeak 750. Medium metabolites were separated using reverse phase chromatography (Kinetex C18, 100 mm * 2.1 mm, 2.6 µM 100 Å, Phenomenex). For reversed phase elution, solvents were prepared as follows (A) H_2O, 0.1 % formic acid (B) 75:25 acetonitrile: isopropanol, 0.1% formic acid. All solvents were of HPLC grade. Linear gradients were devised as follows for reversed phase separation (0.5 ml/minute) minute 0: 5%B, minute 8: 95%B, minute 10: 95%B, minute 10.2: 5%B, minute 12: 5%B. Data was analyzed using Mass Hunter Qual (Agilent) using the "find by formula" function with a match tolerance for masses of 10 ppm and for retention times of 0.35 min. Metabolites were identified using synthetic standards.

2.8 Data analyses

All data were analyzed as indicated and visualized using GraphPad Prism version 8 for Windows (GraphPad Software, San Diego California USA, www.graphpad.com).

3. Results

3.1 Production of 3HDec in media of E. coli stationary growth phase

It is still under debate whether MCFAs are the endogenous agonists of GPR84, since so far their presence in relevant tissues at appropriate concentrations remains to be demonstrated [19]. However, 3-hydroxy MCFAs, including 3-hydroxydecanoic acid (3HDec), which has previously been shown to exert agonistic activity at both HCA_3 and GPR84, are components of lipopolysaccharides (LPS) in Gram-negative bacteria and used as endotoxin markers in clinical samples [10]. An *in vitro* approach was chosen to determine, whether 3-hydroxy MCFAs are present in the growth media of Gram-negative bacteria. We sampled media from different phases of the growth curve of the gram-negative *E. coli* K-12 MG1655 strain (Figure 1A). The relative concentration of the 3-hydroxy MCFAs, 3HDec, 3-hydroxylauric acid (3HLau) and 3-hydroxymyristic acid (3HMyr) was measured and found to be increased over time, with the highest levels in the stationary phase of the *E. coli* cultures (Figure 1B).

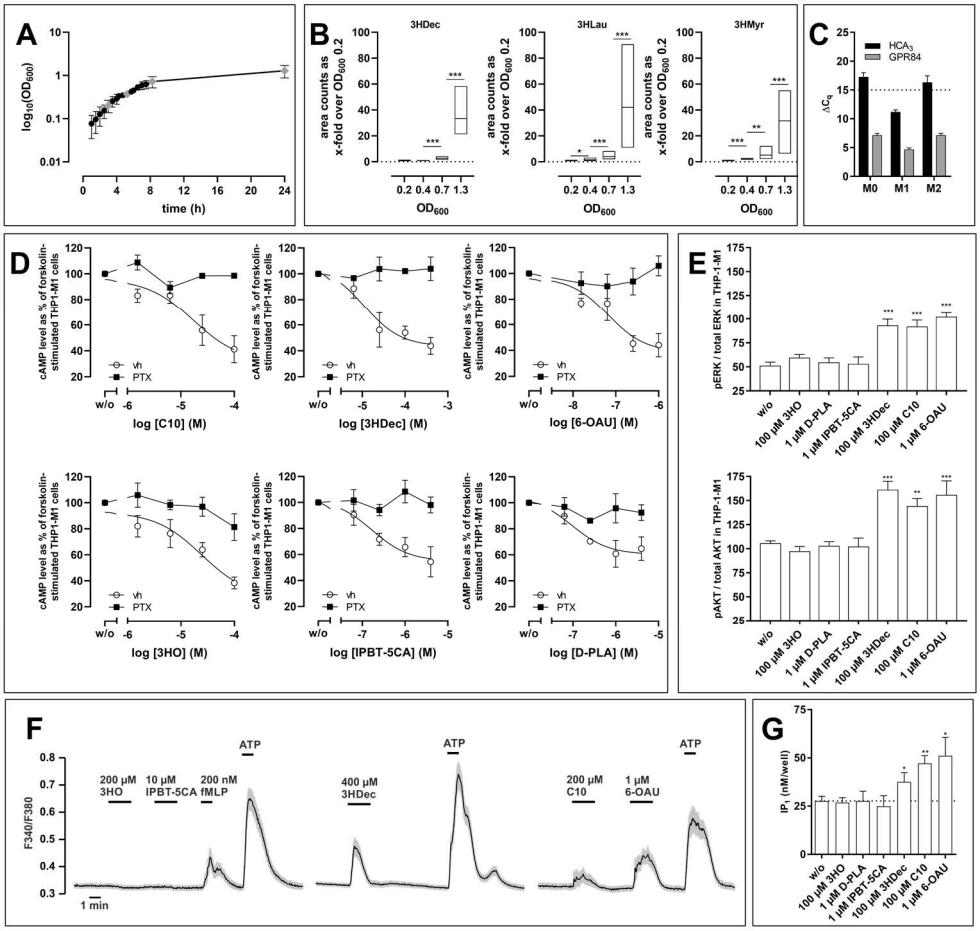

Figure 1: 3-hydroxy medium chain fatty acid concentration is increased in *E. coli* growth medium. HCA_3 and GPR84 are functionally expressed in THP-1-M1 macrophages.

(A) OD_{600} of *E. coli* K-12 MG1655, cultured in M9 mineral medium was determined (mean ± SEM, n = 2 experiments, each 5 replicates). At the time points highlighted in grey, samples corresponding to ~ 20 mg *E. coli* wet weight were taken and centrifuged. (B) 250 µl of the resulting supernatant medium were extracted and analyzed using LC-MS. Shown are the relative concentrations, i.e. area counts under the curves (each as x-fold of values obtained for sample OD_{600} = 0.2) shown as min to max with line at mean for 3-hydroxydecanoic acid (3HDec), 3-hydroxylauric acid (3HLau) and 3-hydroxymyristic acid (3HMyr). (C) The mRNA expression of HCA_3 and GPR84 in THP-1 cells differentiated to M0-, M1- or M2-like macrophages (n = 3, reference gene ACTB C_q = 16) is shown as ΔC_q-values (mean ± SEM). (D) cAMP inhibitory signaling induced by HCA_3 and GPR84 agonists was examined in THP-1-M1 macrophages in absence (w/o = 2.5 ± 0.3 nM cAMP/well is set 100%) and presence of PTX (w/o = 8.0 ± 1.5 nM cAMP/well is set 100% and shown as mean ± SEM, n = 3). (E) Agonist-induced phosphorylation of endogenous ERK 1/2 and AKT1/2/3 in cellular lysates of THP-1-M1 macrophages stimulated with HCA_3 and GPR84 agonists mean ± SEM (n ≥ 3). (F) Fura 2-based Ca^{2+} imaging experiments were performed in non-transfected THP-1-M1 macrophages. The fluorescence ratio (F340/F380) represents the time course of the intracellular Ca^{2+} concentration. Each trace represents the average Ca^{2+} signal ± SEM of 31-35 cells derived from single experiments. (G) Intracellular IP_1 levels in response to HCA_3 and GPR84 agonists as mean ± SEM (n = 5). (B, E, G) Statistical analyses were performed applying paired two-tailed t-tests. * $P \leq 0.05$; ** $P \leq 0.01$; *** $P \leq 0.001$.

3.2 HCA_3 and GPR84 are highly expressed and functionally active in THP-1-derived inflammatory macrophages

As previously shown, 3HDec activates the $G\alpha_i$-coupled receptors, HCA_3 and GPR84 [5], which are often co-expressed in innate immune cells, namely monocytes, macrophages and neutrophils (PMNs). Here, we established differentiated and polarized THP-1 cells as a macrophage model to study HCA_3 and GPR84. Highest mRNA expression of both, HCA_3 and GPR84, was found in THP-1 cells polarized to M1-like macrophages (referred to as THP-1-M1) (Figure 1C). We performed cyclic AMP (cAMP) inhibition assays in absence and presence of

the $G\alpha_{i/o}$-protein inhibitor pertussis toxin (PTX). All tested GPR84 agonists (C10, 6-n-octylaminouracil (6-OAU)) and HCA_3 agonists (3HO, D-PLA, IPBT-5CA) as well as the common agonist 3HDec induced a PTX-sensitive reduction of intracellular cAMP levels (Figure 1D). Previously, we demonstrated ERK activation in non-immune cells with heterologously expressed HCA_3 or GPR84 [5]. However, in THP-1-M1 macrophages, only GPR84-activating agonists (C10, 3HDec, 6-OAU) but not the HCA_3-specific agonists (3HO, D-PLA, IPBT-5CA) increased pERK/total ERK and pAKT/total AKT ratios (Figure 1E). Further, Ca^{2+} imaging experiments in single THP-1-M1 cells were performed to investigate the involved signaling components. The compounds, N-formylmethionyl-leucyl-phenylalanine (fMLP) and ATP, used to verify general responsiveness of the cells, evoked moderate or strong Ca^{2+} responses (Figure 1F). The GPR84 agonist C10, the most potent GPR84 agonist 6-OAU, and the shared agonist 3HDec induced moderate and graded Ca^{2+} elevations while the HCA_3 agonists (3HO, IPBT-5CA) failed to evoke Ca^{2+} signals (Figure 1F). Ca^{2+} mobilization can be induced by inositol phosphate, which is produced upon activation of $G\alpha_{q/11}$ protein-coupled receptors. Hematopoietic cells specifically express the $G\alpha_{15}$ protein (GNA15), which belongs to the $G\alpha_{q/11}$ protein family. Thus, inositol monophosphate (IP_1) accumulation as a measure for phospholipase C (PLC) activity downstream of $G\alpha_{q/11}$/$G\alpha_{15}$ signaling was measured [20,21]. Again, only C10, 6-OAU and 3HDec induced a significant increase in IP_1 levels (Figure 1G).

3.3 GPR84 couples to the $G\alpha_{15}$ protein, causing ERK activation, IP_1 accumulation and Ca^{2+} signaling in inflammatory macrophages

To determine receptor-specificity of the activated signaling components, we transfected THP-1-M1 macrophages with siRNA targeting HCA_3, GPR84 or $G\alpha_{15}$ mRNA (siGNA15). Successful knockdown was confirmed using RT-qPCR although only about 40 % reduction of GPR84 mRNA expression could be achieved as compared to 60 % for HCA_3 and 70 % for $G\alpha_{15}$ (Figure 2A). No specific high quality antibody targeting GPR84 or HCA_3 are available. To test whether reduced GPR84 and HCA_3 mRNA levels translate to decreased protein expression, we used HEK293-T cells, which do not express either receptor endogenously. We co-transfected HEK293-T cells with plasmids encoding HA-tagged HCA_3 or HA-tagged GPR84 in combination with receptor-specific siRNA or siNC. Cell surface expression of the HA-tagged HCA_3 protein was about 60 % decreased in presence of $siHCA_3$ as compared to siNC, while cell surface expression of HA-tagged GPR84 protein was about 40 % decreased in presence of siGPR84 as compared to siNC (Figure S1). Using cAMP inhibition assays, both HCA_3 agonists (3HO, D-PLA) caused a reduction of intracellular cAMP levels that was abolished by siRNA-mediated knockdown of HCA_3 ($siHCA_3$) (Figure 2B). Despite limited efficacy, siRNA-mediated knockdown of GPR84 significantly inhibited the C10- and 6-OAU-induced reduction of intracellular cAMP levels while knockdown of HCA_3 had no effect (Figure 2B). The 3HDec-mediated decrease in cAMP levels was partially inhibited by $siHCA_3$ or siGPR84, respectively (Figure 2B). Next, we tested the PTX sensitivity as well as involvement of GPR84, HCA_3 and $G\alpha_{15}$ in ERK and AKT phosphorylation. ERK phosphorylation induced by GPR84 agonists was reduced in presence of PTX and abolished when cells were transfected with siGPR84 or siGNA15 (Figure 2C). Pre-incubation with PTX caused a complete loss, while siGPR84 but not siGNA15 caused a reduction of GPR84 agonist-mediated AKT activation (Figure 2D). Thus, although knockdown efficiency of GPR84 did not exceed 40 %, the significant loss of signaling upon activation by the GPR84-specific surrogate agonist 6-OAU (Figures 2C, 2D) supports that the GPR84 level is sufficiently reduced by the siRNA used. To test the involvement of $G\alpha_{15}$ in Ca^{2+} signaling, the GPR84-specific surrogate agonist 6-OAU, which induces maximal Ca^{2+} responses, was used for measurements in non-transfected, siNC-transfected (negative control siRNA) and siGNA15-transfected THP-1-M1 macrophages.

Knockdown of $G\alpha_{15}$ inhibited the 6-OAU-induced Ca^{2+} responses whereas siNC had no effect (Figure 2E).

In summary, GPR84, a receptor known to couple exclusively to $G\alpha_{i/o}$ proteins [22], but not HCA_3, transduces its signals in THP-1-M1 macrophages also via the $G\alpha_{15}$ protein, a hitherto unknown characteristic.

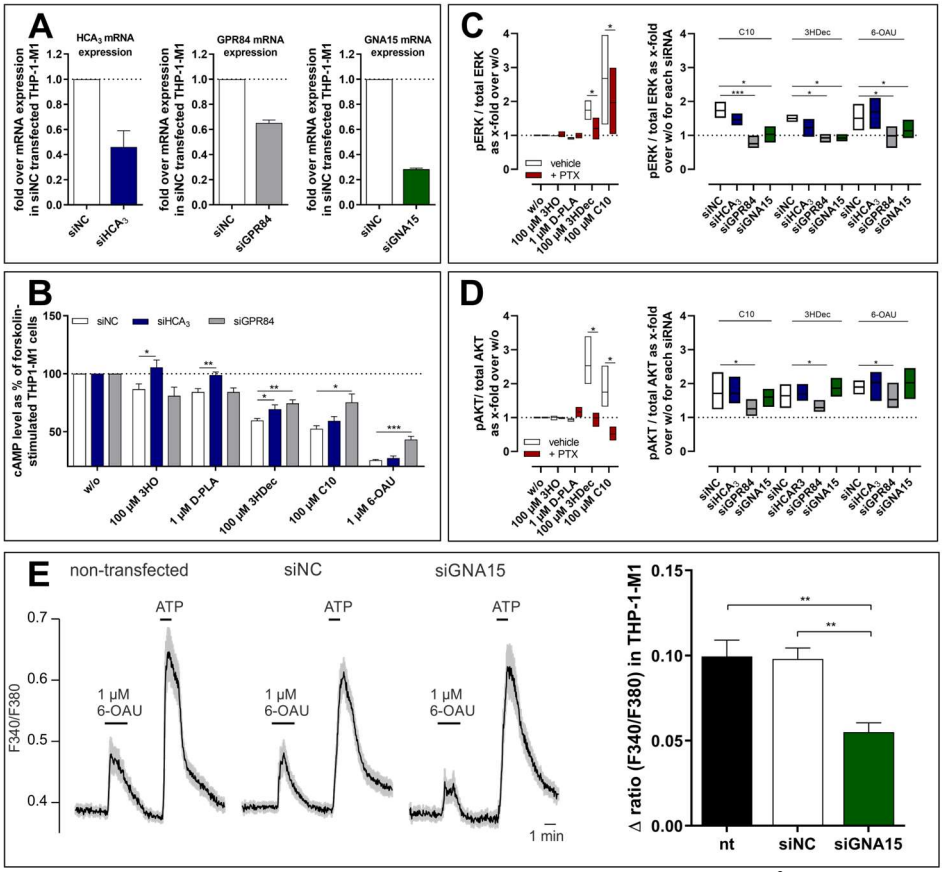

Figure 2: Activation of GPR84 causes $G\alpha_{15}$-mediated ERK activation and Ca^{2+} signaling in THP-1-M1 macrophages.

(A) THP-1-M1 macrophages were transfected with either $siHCA_3$, siGPR84, siGNA15 (targeting $G\alpha_{15}$-mRNA) or siNC (negative Ctrl siRNA), which caused ~ 60 %, ~ 40 % and ~ 70 % reduction in respective mRNA levels as detected using RT-qPCR. (B) cAMP inhibitory signaling induced by HCA_3 and GPR84 agonists was examined in THP-1-M1 macrophages after transfection with $siHCA_3$, siGPR84 or siNC. Agonist-induced phosphorylation of endogenous ERK 1/2 (C) and AKT1/2/3 (D) were measured in cellular lysates of THP-1-M1 macrophages in absence and presence of PTX or macrophages transfected with siNC, $siHCA_3$, siGPR84 and siGNA15, w/o was set 1, respectively. (E) 1 µM of the GPR84-specific surrogate agonist 6-OAU induced a similar Ca^{2+} signal in non-transfected and siNC-transfected cells, which was diminished in siGNA15-transfected cells, while the ATP-induced Ca^{2+} response was not visibly affected. The change (Δ) in the fluorescence ratio (F340/F380) for the 6-OAU-induced Ca^{2+} signals in non-transfected (nt), siNC- and siGNA15-transfected cells is depicted as mean ± SEM from n = 4 experiments per group (each experiment containing 37 - 47 cells). Data is shown as (A, B) mean ± SEM (C, D) min to max with line at mean (n = 3 to 6 independent experiments). Statistical analyses were performed applying unpaired t-tests. * $P \leq 0.05$; ** $P \leq 0.01$; *** $P \leq 0.001$.

3.4 GPR84 triggers tumor necrosis factor α (TNFα) secretion, activation of nuclear factor κ B (NFκB) and NADPH oxidase-dependent ROS production in inflammatory macrophages

It was previously shown in mouse M1 macrophages that GPR84 activation by 6-OAU results in activation of NFκB and increases TNFα levels [6]. We confirmed this effect in human THP-1-M1 macrophages and found that stimulation with C10, 3HDec and 6-OAU increased the release of TNFα, whereas only C10 and 6-OAU, but not 3HDec activated NFκB (Figures S2A, S2B).

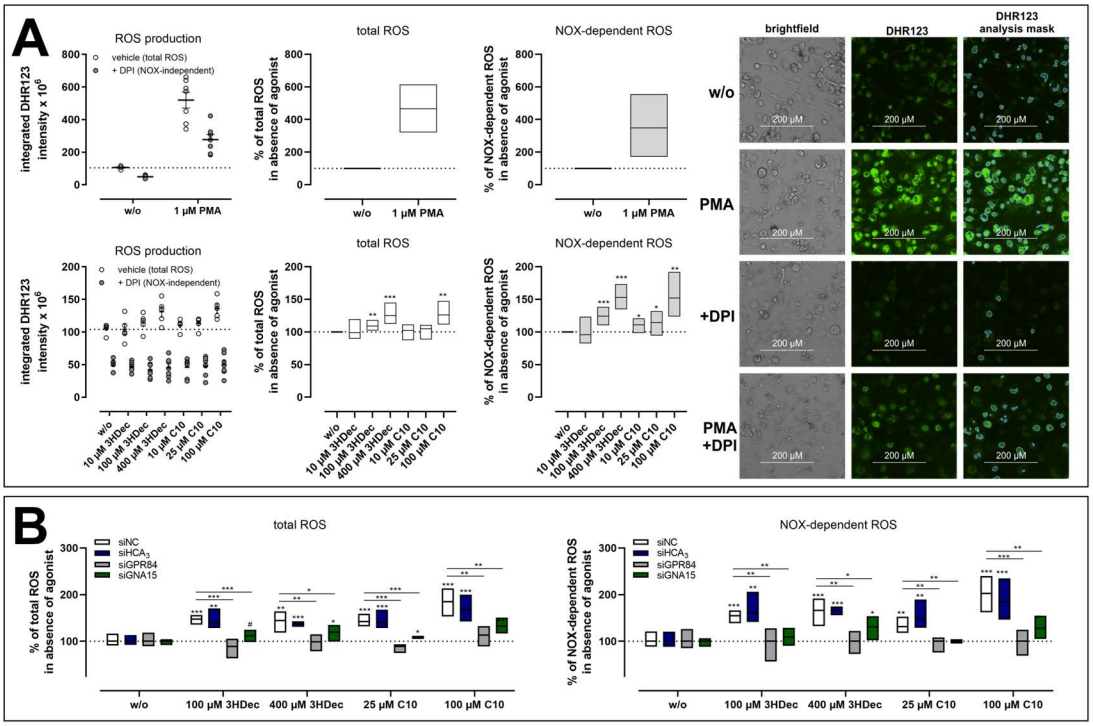

Figure 3: GPR84 agonists stimulate NADPH oxidase-dependent ROS production in inflammatory macrophages.

(A) Production of reactive oxygen species (ROS) in THP-1-M1 macrophages was examined by adding DHR123 (dihydrorhodamine 123) to the cells and assessing differences in the intracellular DHR123 fluorescence intensity after incubation with GPR84 agonists in the absence and presence of the NADPH-oxidase (NOX) inhibitor diphenyleneiodonium chloride (DPI, 4 µM). PMA was used as a positive control. Representative images and analyses performed using the Celigo Imaging Cytometer are shown. The sum of green pixel intensities in all segmented cells per well, correlating to DHR123 integrated intensity in the absence (measure for overall ROS-production) and presence of DPI (measure for NOX-independent ROS-production) was used to determine total ROS and NOX-dependent ROS-production (n = 7). (B) THP-1-M1 macrophages were transfected with either $siHCA_3$, siGPR84, siGNA15 or siNC. ROS and NOX-dependent ROS was determined (n = 5) (A, B) Green pixel intensities in absence of agonist were set 100 %. Normalized total ROS and NOX-dependent ROS is shown as floating bars min to max, line at mean. Statistical analyses were performed applying an unpaired t-test. * $P \leq 0.05$; ** $P \leq 0.01$; *** $P \leq 0.001$.

Both, TNFα and NFκB signaling are known to be associated with the production of reactive oxygen species (ROS) [23,24]. The enzyme NADPH oxidase (NOX) is crucial for ROS production in immune cells as part of the defense mechanism against invading pathogens [25]. We measured intracellular ROS production in THP-1-M1 macrophages using dihydrorhodamine 123 (DHR123). In cells stimulated with GPR84 agonists for 24 h, the DHR123 intensity was lower in the presence of the NADPH oxidase inhibitor diphenyleneiodonium chloride (DPI), indicating NOX-dependent production of ROS (Figures 3A). To test for differences in the overall intracellular ROS production, we analyzed DHR123 intensity in the absence of DPI. 3HDec and C10 increased total and NOX-mediated ROS formation in THP-1-M1 macrophages, as did the positive control compound phorbol 12-myristate 13-acetate (PMA), but not 6-OAU (Figures 3A, S2C). To determine, whether the 3HDec- and C10-induced increase in total and NOX-dependent ROS was evoked by GPR84 and $G\alpha_{15}$, siRNA-mediated knockdown experiments were performed (Figure 3B). These analyses revealed, despite knockdown efficiency of only 40 %, that solely GPR84 caused the increase in ROS upon stimulation with 3HDec and C10 (Figure 3B). Furthermore, the ROS production in presence of 3HDec and C10 was significantly reduced in macrophages transfected with siGNA15, but was still increased compared to the control, suggesting that $G\alpha_{15}$ is mainly but not exclusively responsible for this effect (Figure 3B).

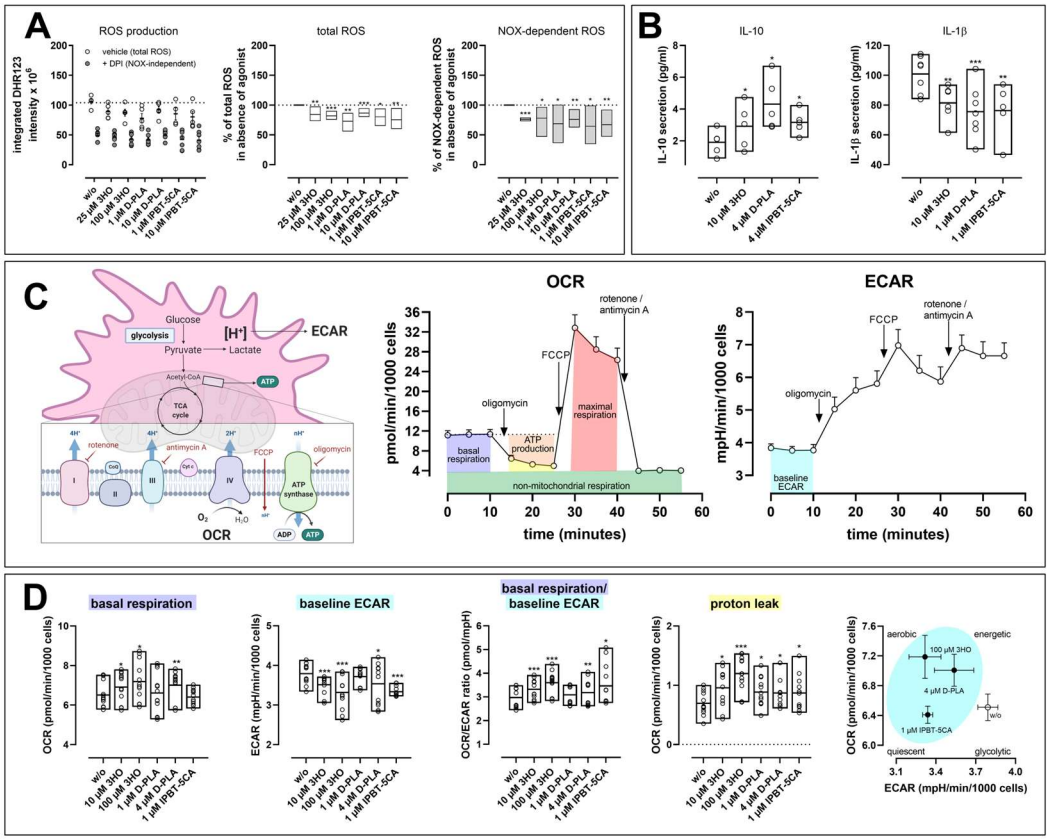

Figure 4: HCA_3 agonists decrease ROS production and IL-1β secretion but increase IL-10 secretion and enhance cellular respiration in THP-1-M1 macrophages.
(A) Production of reactive oxygen species (ROS) in THP-1-M1 macrophages after incubation with HCA_3 agonists in the absence and presence of the NADPH-oxidase (NOX) inhibitor diphenyleneiodonium chloride (DPI, 4 µM) (mean ± SEM of n = 7). Normalized total ROS and NOX-dependent ROS is shown as min to max, line at mean. (B) IL-1β and IL-10 concentrations (in pg/ml, min to max, line at mean of n ≥ 4 biological replicates) in cell culture supernatants of THP-1-M1 macrophages stimulated with HCA_3 agonists. (C) The components of the electron transport chain are localized in mitochondria and the oxygen consumption rate (OCR) and extracellular acidification rate (ECAR) were analyzed in THP-1-M1 macrophages (created using BioRender.com). (D) Shown are metabolic parameters calculated from the OCR and ECAR measurements as described in Material and Methods. Data depicted as floating bars min to max, line at mean of 3 time points of 4 independent experiments (n = 12), each carried out in 4 technical replicates. Statistical analyses (w/o versus agonists) were performed using a repeated measures One-Way ANOVA * $P \leq 0.05$; ** $P \leq 0.01$; *** $P \leq 0.001$.

3.5 HCA_3 triggers anti-inflammatory signaling via reduction of ROS production and IL-1β secretion but increase of IL-10 secretion and cellular respiration in inflammatory macrophages

In contrast to GPR84 agonists, HCA_3 activation had no effect on NFκB activation or TNFα secretion (Figures S2A, S2B), but caused a significant decrease in total and NOX-dependent ROS levels, suggesting an anti-inflammatory action (Figure 4A). In contrast to GPR84, little is known about HCA_3-mediated immune cell functions. To further elucidate the potential anti-inflammatory role of HCA_3, we analyzed the effect of HCA_3 agonists on the secretion of IL-10, an anti-inflammatory cytokine and IL-1β, a pro-inflammatory cytokine in THP-1-M1 macrophages. IL-1β concentrations in the supernatant were significantly reduced, when cells were stimulated with the HCA_3 agonists 3HO, D-PLA or IPBT-5CA (surrogate HCA_3-specific agonist), while IL-10 release was significantly increased (Figure 4B). Cellular metabolism and macrophage function are tightly linked and IL-10 has been shown to inhibit inflammation-induced glycolysis while promoting oxidative phosphorylation in macrophages [16,26]. We performed metabolic flux analyses using the Seahorse Mito Stress Test (Agilent). Oxygen consumption rate (OCR) and extracellular acidification rate (ECAR) were measured in

THP-1-M1 macrophages stimulated with HCA_3 agonists in the absence and presence of selective inhibitors of the electron transport chain (ETC) (Figure 4C). HCA_3 agonists caused an increase in basal respiration, associated with an increased proton leakage, but not ATP production (Figures 4D, S3). This is accompanied by a decreased basal ECAR indicating a lower glycolytic rate. This resulted in a significantly increased ratio of basal respiration/ECAR but reduced spare respiratory capacity (Figures 4D, S3). HCA_3 agonists affected neither maximal respiration nor non-mitochondrial oxygen consumption (Figure S3).
In summary, this indicates that HCA_3 activation enhances aerobic respiration (oxidative phosphorylation), while the rate of glycolysis is reduced. This is a characteristic metabolic feature associated with anti-inflammatory responses of macrophages [16]. Macrophages are mostly tissue-resident descendants of circulating monocytes. The most abundant circulating leukocytes in humans and the first responders to an infection are neutrophils [27]. Thus, we analyzed the role of HCA_3 and GPR84 for neutrophil function.

3.6 HCA_3 stimulation counteracts GPR84-induced PMN activation

In PMNs, high mRNA expression of both receptors and functional presence using dynamic mass redistribution (DMR) measurements was verified (Figures 5A, 5B). DMR is a label-free technique and therefore highly suitable for signaling analysis in primary cells to determine time-resolved receptor activation independent of second messenger levels. Stimulation of PMNs with all HCA_3 agonists resulted in DMR responses completely suppressed by PTX, indicating coupling to $G\alpha_{i/o}$-proteins (Figure 5B). Both, 3HDec and C10, induced a partially PTX-insensitive DMR response, suggesting involvement of additional signaling pathways apart from $G\alpha_{i/o}$ stimulation (Figure 5B). Furthermore, GPR84 agonists activated ERK but not AKT in PMNs (Figure S4A).
PMNs are the most abundant circulating leukocytes in humans and able to form neutrophil extracellular traps (NET) [28]. Released DNA, reflecting NET formation, can be stained with propidium iodide (PI) [29]. Here, the ratio of cell counts positive for PI and for Hoechst 33342 (total cell number) derived from image-based analyses were used to quantify activation of PMNs (Figures 5C, S4B). C10 and 3HDec induced a significant increase in activated PMNs (Figure 5C). PMA served as positive control and resulted in almost 100 % activation, reflected by a ratio of PI count/Hoechst 33342 count of ~1 (Figure 5C). Some GPCRs in immune cells amplify or counteract signals induced by other receptors. We found that presence of the HCA_3-specific agonists D-PLA and IPBT-5CA caused a significant reduction of the 3HDec- or C10-induced PMN activation (Figure 5C).
NET formation can be lytic, leading to cell death (suicidal NETosis) or resulting in the formation of functional anuclear cytoplasts capable of phagocytosis (vital NETosis) [30,31]. We analyzed the effect of HCA_3 or GPR84 stimulation on phagocytic activity of PMNs by treatment with HCA_3 agonists, GPR84 agonists or PMA (positive control) and subsequent addition of pHrodo Red-conjugated *E. coli* particles (Figure 5D). These particles show pH-sensitive fluorescence upon ingestion into acidic phagosomes. The actin cytoskeleton was stained using Alexa Fluor 488-labeled phalloidin while the nuclei were stained with Hoechst 33342 (Figure 5D). Automatic image-based analyses were performed to determine: (1) the number of cell bodies (green), containing (blue) or lacking an intact nucleus, (2) the number of phagocytic cells (green and red), and (3) the average number of particles per cell (red per green cell body) (Figure 5D).
Upon stimulation with C10, 3HDec or the positive control PMA a reduced number of cells were containing nuclei consequently leading to an increased number of cells lacking nuclei (Figure 5D). Additionally, the same treatments lead to a significantly decreased number of phagocytic cells, i.e. of cell bodies containing *E. coli* particles (Figure 5D). At last, the number of particles ingested per phagocytic cell was determined. Although we detected a lower number of

phagocytic cells when PMNs were stimulated with 3HDec or C10, we found a significantly higher number of ingested particles per cell body under these conditions (Figure 5D).
C10 and 3HDec induce both suicidal NETosis (Figure 5C) and vital NETosis, supported by the increased phagocytic capacity (Figures 5D).

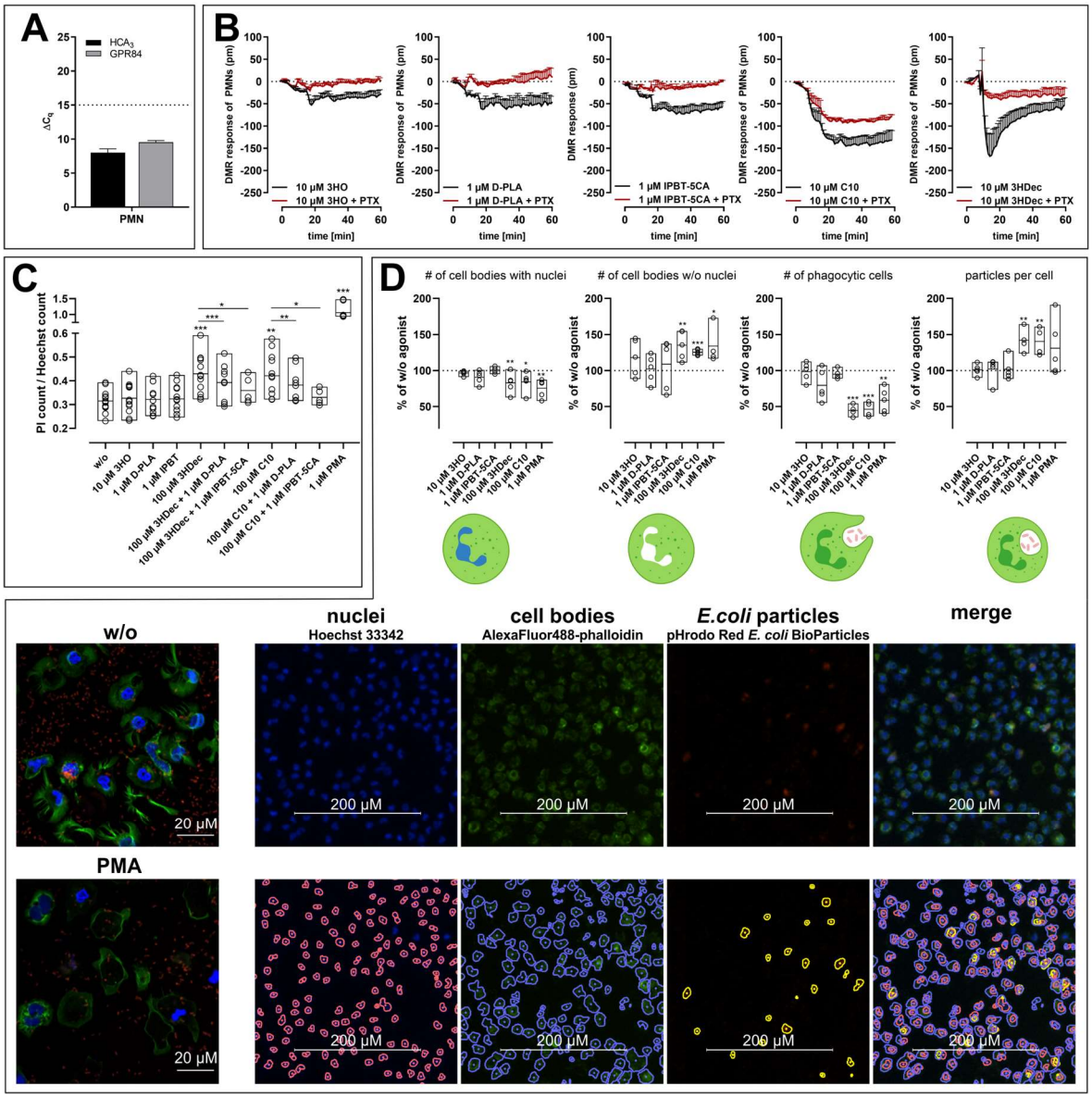

Figure 5: C10 and 3HDec induce activation of primary human neutrophils, counteracted by HCA_3 agonists. (A) The mRNA expression of HCA_3 and GPR84 in freshly isolated human PMNs (n = 4 different donors, reference genes ACTB C_q = 16 and B2M C_q = 17) is shown as ΔC_q-values (mean ± SEM, each sample measured in duplicates). (B) Dynamic mass redistribution (DMR) responses in PMNs (mean ± SEM of n = 4 different donors) upon stimulation with HCA_3 and GPR84 agonists with or without PTX preincubation. (C) PMNs were incubated with HCA_3, GPR84 agonists or PMA, stained with propidium iodide (PI, red) and Hoechst 33342 (blue). The number of activated (PI) / total cells (Hoechst 33342) was determined. (D) PMN nuclei were stained with Hoechst 33342, cytoskeleton was stained using AlexaFluor488-phalloidin (F-Actin) and phagocytosis of pHrodo Red-conjugated *E. coli* particles was assessed. Data is shown as percent of numbers determined in absence of agonists. (C) n ≥ 10 and (D) n = 5 independent experiments each performed with PMNs of different donors, carried out in triplicates, is shown as min to max, line at mean. Statistical analyses were performed applying paired two-tailed t-test. * $P \leq 0.05$; ** $P \leq 0.01$; *** $P \leq 0.001$. Cell illustrations in D were created with BioRender.com.

4. Discussion

GPR84 and HCA_3 are known to couple to $G\alpha_{i/o}$ proteins and exhibit overlapping expression in monocytes, macrophages and neutrophils (reviewed in [19]). While GPR84 is a widely studied receptor, constituting an attractive pharmacological target for the development of anti-inflammatory drugs, data on HCA_3 function in immune cells is rather scarce. Several surrogate GPR84 ligands have been discovered but little is known about the signaling components involved in the pro-inflammatory effects induced upon GPR84 activation (reviewed in [19]). For HCA_3 on the other hand, a receptor only present in humans and great apes, anti-inflammatory action has been suggested, but more detailed insights are lacking [5]. The 3-hydroxy MCFA 3HDec, a gram-negative bacterial-derived MCFA, activates both GPR84 and HCA_3, which exhibit opposing effects in innate immune cells. Therefore, deciphering GPR84- and HCA_3-activated signaling pathways and their physiological consequences helps to further define their therapeutic potential.

Here, we unraveled the molecular differences in GPR84- and HCA_3-mediated signaling in innate immune cells. We conducted functional analyses to determine consequences for immune cell responses upon activation of those two GPCRs. Regarding the origin of 3HDec, we showed that levels of 3-hydroxy MCFAs strongly accumulate in association with the increasing death of gram-negative bacteria, like *E. coli* (Figure 1B). Previous studies had also shown in other contexts that 3HDec and 3-hydroxy derivatives of other MCFAs are degradation products of LPS [32,33]. In a heterologous expression system we showed recently that signaling kinetics and components involved in signal transduction of GPR84 and HCA_3 differ upon activation by 3HDec [5]. However, here we found that in human macrophages and primary human neutrophils, the HCA_3-dependent signaling upon 3HDec stimulation is negligible, while 3HDec as well as C10 mediate pro-inflammatory signaling through activation of $G\alpha_{15}$-coupled GPR84 (Figures 2B-2E, 3B). To our best knowledge, coupling of GPR84 to $G\alpha_{15}$ in addition to $G\alpha_{i/o}$ has not been described before. In a physiological context, one may speculate that elimination of bacteria by innate immune cells is accompanied by a release of LPS-derived 3-hydroxy MCFAs, causing local concentrations high enough to activate GPR84 followed by recruitment and activation of further immune cells. Thus, it is conceivable that LPS-derived 3-hydroxy MCFAs are the physiological relevant GPR84 agonists. Future analytical studies examining local concentrations of 3-hydroxy MCFAs in infected / inflamed tissue may shed further light on this aspect. It has previously been shown that $G\alpha_{15}$ couples chemoattractant receptors efficiently to PLCβ and NFκB activation [34]. This is in line with our observations of GPR84-mediated increase of intracellular Ca^{2+}, IP_3 and NFκB activation (Figures 1F, 1G, 2E, S2B). Further, we provide evidence for GPR84-, $G\alpha_{15}$-dependent ERK activation and ROS production in macrophages (Figures 2C, 3B, 6). In neutrophils, which are the most abundant circulating leukocytes in humans and the first responders to an infection [27], GPR84 activation with C10 or 3HDec resulted in activation of neutrophils (suicidal NETosis), which is the defining step in the inflammatory response (Figure 5C). At the same time phagocytic capacity (vital NETosis) was increased, further highlighting a role of GPR84 in pro-inflammation (Figures 5D, 6). Several studies already highlighted GPR84 as chemoattractant receptor [6,8,35]. Assuming that neutrophils and macrophages are recruited to the side of bacterial infection due to locally increasing 3HDec levels, GPR84 activation will then lead to $G\alpha_{15}$-dependent NETosis, phagocytosis and ROS production to limit the infection.

HCA_3 signaling, on the contrary, did not affect neutrophil activation/phagocytosis by itself but counteracted GPR84-mediated PMN activation, potentially to prevent damage resulting from excess activation of PMNs (Figures 5C, 6). Thus, HCA_3 may be especially important for balancing the response of innate immune cells at the site of a bacterial infection. HCA_3 tones down pro-inflammatory IL-1β secretion and ROS production, but increases anti-inflammatory IL-10 secretion from macrophages (Figures 4A, 4B, 6). This is a potential mechanism to prevent

excessive damage of surrounding tissue and/or to help resolve the inflammation by reducing the recruitment of further immune cells through lowering cytokine release [36]. Cellular metabolism is tightly linked to macrophage function and the activity of various metabolic pathways is linked to pro- or anti-inflammatory signaling [37]. From an immunometabolic point, HCA_3 activation caused a decrease in glycolytic activity but increase in oxidative phosphorylation (Figures 4D). This kind of metabolic phenotype is rather associated with anti-inflammatory responses, while pro-inflammation is usually accompanied by strong dependence on glycolysis (reviewed in [16]). LAB-derived metabolites, like e.g. D-PLA activating HCA_3, are also known to exhibit anti-bacterial and anti-fungal properties rendering the presence of pathogenic microbes in LAB-fermented food, like Sauerkraut, less likely [38,39]. In this scenario, it appears reasonable to speculate that HCA_3 activated by D-PLA induces a hyporesponsiveness in neutrophils and macrophages, preventing excessive cytokine release and therefore inflammation.

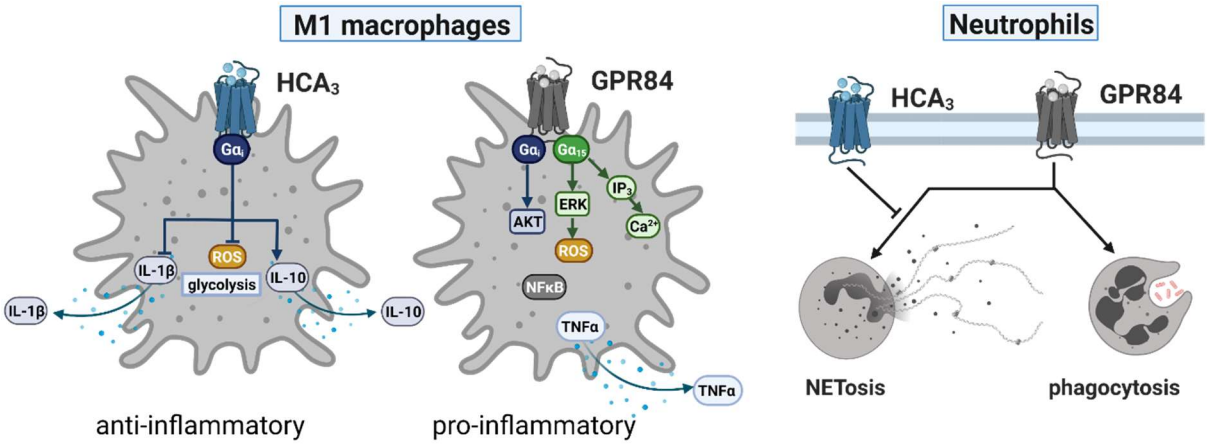

Figure 6: GPR84 and HCA_3 regulate innate immune cell functions.
THP-1-M1 macrophages and primary human neutrophils express both, GPR84 and HCA_3. HCA_3 is exclusively coupled to $G\alpha_{i/o}$. Activation of HCA_3 results in decreased IL-1β but increased IL-10 secretion. Less ROS are produced and macrophage metabolism shifts to a less glycolytic phenotype in presence of HCA_3 agonists. GPR84 is coupled to $G\alpha_{i/o}$ and $G\alpha_{15}$ in THP-1-M1 macrophages. Activation of GPR84 causes $G\alpha_{15}$-dependent ERK activation and increases intracellular Ca^{2+} and IP_3 levels. NFκB activation, TNFα secretion and formation of ROS are increased upon stimulation of GPR84. GPR84 agonists cause neutrophil activation and enhanced phagocytosis, which is inhibited in presence of HCA_3 agonists (created with BioRender.com).

5. Conclusions

In conclusion, we provide new insights into the molecular regulation of innate immune cells by HCA_3 and GPR84 (Figure 6). We propose that both receptors can serve as new targets to tackle chronic inflammation. Our discovery of $G\alpha_{15}$ as a crucial mediator of GPR84-induced pro-inflammatory signaling provides a key step towards a better assessment of the potential of GPR84 as drug target. Future studies shall focus on this aspect to determine potency and efficacy of GPR84-targeting ligands.

6. Acknowledgements

This work was supported by the German Research Foundation (Project number 407707190), by the European Social Funds and research funding of the Medical Faculty, University Leipzig. We thank Torsten Schöneberg for critical reading and commenting on the manuscript.

7. References

[1] J. Wang, X. Wu, N. Simonavicius, H. Tian, L. Ling, Medium-chain fatty acids as ligands for orphan G protein-coupled receptor GPR84, J. Biol. Chem. 281 (2006) 34457–34464. https://doi.org/10.1074/jbc.M608019200.

[2] K. Ahmed, S. Tunaru, C.-D. Langhans, J. Hanson, C.W. Michalski, S. Kölker, P.M. Jones, J.G. Okun, S. Offermanns, Deorphanization of GPR109B as a receptor for the beta-oxidation intermediate 3-OH-octanoic acid and its role in the regulation of lipolysis, J. Biol. Chem. 284 (2009) 21928–21933. https://doi.org/10.1074/jbc.M109.019455.

[3] A. Peters, P. Krumbholz, E. Jäger, A. Heintz-Buschart, M.V. Çakir, S. Rothemund, A. Gaudl, U. Ceglarek, T. Schöneberg, C. Stäubert, Metabolites of lactic acid bacteria present in fermented foods are highly potent agonists of human hydroxycarboxylic acid receptor 3, PLoS Genet. 15 (2019) e1008145. https://doi.org/10.1371/journal.pgen.1008145.

[4] Y. Irukayama-Tomobe, H. Tanaka, T. Yokomizo, T. Hashidate-Yoshida, M. Yanagisawa, T. Sakurai, Aromatic D-amino acids act as chemoattractant factors for human leukocytes through a G protein-coupled receptor, GPR109B, Proc. Natl. Acad. Sci. U. S. A. 106 (2009) 3930–3934. https://doi.org/10.1073/pnas.0811844106.

[5] A. Peters, P. Rabe, P. Krumbholz, H. Kalwa, R. Kraft, T. Schöneberg, C. Stäubert, Natural biased signaling of hydroxycarboxylic acid receptor 3 and G protein-coupled receptor 84, Cell Commun Signal 18 (2020) 31. https://doi.org/10.1186/s12964-020-0516-2.

[6] C. Recio, D. Lucy, G.S.D. Purvis, P. Iveson, L. Zeboudj, A.J. Iqbal, D. Lin, C. O'Callaghan, L. Davison, E. Griesbach, A.J. Russell, G.M. Wynne, L. Dib, C. Monaco, D.R. Greaves, Activation of the Immune-Metabolic Receptor GPR84 Enhances Inflammation and Phagocytosis in Macrophages, Front. Immunol. 9 (2018) 1419. https://doi.org/10.3389/fimmu.2018.01419.

[7] M. Suzuki, S. Takaishi, M. Nagasaki, Y. Onozawa, I. Iino, H. Maeda, T. Komai, T. Oda, Medium-chain fatty acid-sensing receptor, GPR84, is a proinflammatory receptor, J. Biol. Chem. 288 (2013) 10684–10691. https://doi.org/10.1074/jbc.M112.420042.

[8] D. Lucy, G.S.D. Purvis, L. Zeboudj, M. Chatzopoulou, C. Recio, C.J.R. Bataille, G.M. Wynne, D.R. Greaves, A.J. Russell, A Biased Agonist at Immunometabolic Receptor GPR84 Causes Distinct Functional Effects in Macrophages, ACS Chem. Biol. 14 (2019) 2055–2064. https://doi.org/10.1021/acschembio.9b00533.

[9] S. Offermanns, S.L. Colletti, T.W. Lovenberg, G. Semple, A. Wise, A.P. IJzerman, International Union of Basic and Clinical Pharmacology. LXXXII: Nomenclature and Classification of Hydroxy-carboxylic Acid Receptors (GPR81, GPR109A, and GPR109B), Pharmacol. Rev. 63 (2011) 269–290. https://doi.org/10.1124/pr.110.003301.

[10] B. Szponar, E. Norin, T. Midtvedt, L. Larsson, Limitations in the use of 3-hydroxy fatty acid analysis to determine endotoxin in mammalian samples, Journal of microbiological methods 50 (2002) 283–289. https://doi.org/10.1016/s0167-7012(02)00038-6.

[11] E. Kolaczkowska, P. Kubes, Neutrophil recruitment and function in health and inflammation, Nat Rev Immunol 13 (2013) 159–175. https://doi.org/10.1038/nri3399.

[12] P. Italiani, D. Boraschi, From Monocytes to M1/M2 Macrophages: Phenotypical vs. Functional Differentiation, Front. Immunol. 5 (2014) 514. https://doi.org/10.3389/fimmu.2014.00514.

[13] D.C. Dale, L. Boxer, W.C. Liles, The phagocytes: neutrophils and monocytes, Blood 112 (2008) 935–945. https://doi.org/10.1182/blood-2007-12-077917.

[14] D.M. Mosser, J.P. Edwards, Exploring the full spectrum of macrophage activation, Nat Rev Immunol 8 (2008) 958–969. https://doi.org/10.1038/nri2448.

[15] E. Mortaz, S.D. Alipoor, I.M. Adcock, S. Mumby, L. Koenderman, Update on Neutrophil Function in Severe Inflammation, Front. Immunol. 9 (2018) 2171. https://doi.org/10.3389/fimmu.2018.02171.
[16] A. Viola, F. Munari, R. Sánchez-Rodríguez, T. Scolaro, A. Castegna, The Metabolic Signature of Macrophage Responses, Front. Immunol. 10 (2019) 1462. https://doi.org/10.3389/fimmu.2019.01462.
[17] D.B. Kuhns, D.A.L. Priel, J. Chu, K.A. Zarember, Isolation and Functional Analysis of Human Neutrophils, Curr. Protoc. Immunol. 111 (2015) 7.23.1-7.23.16. https://doi.org/10.1002/0471142735.im0723s111.
[18] M. Genin, F. Clement, A. Fattaccioli, M. Raes, C. Michiels, M1 and M2 macrophages derived from THP-1 cells differentially modulate the response of cancer cells to etoposide, BMC Cancer 15 (2015) 577. https://doi.org/10.1186/s12885-015-1546-9.
[19] V.B. Luscombe, D. Lucy, C.J.R. Bataille, A.J. Russell, D.R. Greaves, 20 Years an Orphan: Is GPR84 a Plausible Medium-Chain Fatty Acid-Sensing Receptor?, DNA and cell biology 39 (2020) 1926–1937. https://doi.org/10.1089/dna.2020.5846.
[20] N. Mizuno, H. Itoh, Functions and regulatory mechanisms of Gq-signaling pathways, Neurosignals. 17 (2009) 42–54. https://doi.org/10.1159/000186689.
[21] D. Billups, B. Billups, R.A.J. Challiss, S.R. Nahorski, Modulation of Gq-protein-coupled inositol trisphosphate and Ca2+ signaling by the membrane potential, J. Neurosci. 26 (2006) 9983–9995. https://doi.org/10.1523/JNEUROSCI.2773-06.2006.
[22] S.P. Alexander, J. Battey, H.E. Benson, R.V. Benya, T.I. Bonner, A.P. Davenport, S. Eguchi, A. Harmar, N. Holliday, R.T. Jensen, S. Karnik, E. Kostenis, W.C. Liew, A.E. Monaghan, C. Mpamhanga, R. Neubig, A.J. Pawson, J.-P. Pin, J.L. Sharman, M. Spedding, E. Spindel, L. Stoddart, L. Storjohann, W.G. Thomas, K. Tirupula, P. Vanderheyden, Class A Orphans (version 2019.5) in the IUPHAR/BPS Guide to Pharmacology Database, GtoPdb CITE 2019 (2019). https://doi.org/10.2218/gtopdb/F16/2019.5.
[23] H. Blaser, C. Dostert, T.W. Mak, D. Brenner, TNF and ROS Crosstalk in Inflammation, Trends in cell biology 26 (2016) 249–261. https://doi.org/10.1016/j.tcb.2015.12.002.
[24] M.J. Morgan, Z. Liu, Crosstalk of reactive oxygen species and NF-κB signaling, Cell Res 21 (2011) 103–115. https://doi.org/10.1038/cr.2010.178.
[25] A. Panday, M.K. Sahoo, D. Osorio, S. Batra, NADPH oxidases: an overview from structure to innate immunity-associated pathologies, Cell Mol Immunol 12 (2015) 5–23. https://doi.org/10.1038/cmi.2014.89.
[26] W.K.E. Ip, N. Hoshi, D.S. Shouval, S. Snapper, R. Medzhitov, Anti-inflammatory effect of IL-10 mediated by metabolic reprogramming of macrophages, Science 356 (2017) 513–519. https://doi.org/10.1126/science.aal3535.
[27] K. Prame Kumar, A.J. Nicholls, C.H.Y. Wong, Partners in crime: neutrophils and monocytes/macrophages in inflammation and disease, Cell Tissue Res. 371 (2018) 551–565. https://doi.org/10.1007/s00441-017-2753-2.
[28] V. Brinkmann, U. Reichard, C. Goosmann, B. Fauler, Y. Uhlemann, D.S. Weiss, Y. Weinrauch, A. Zychlinsky, Neutrophil extracellular traps kill bacteria, Science 303 (2004) 1532–1535. https://doi.org/10.1126/science.1092385.
[29] F. Grabcanovic-Musija, A. Obermayer, W. Stoiber, W.-D. Krautgartner, P. Steinbacher, N. Winterberg, A.C. Bathke, M. Klappacher, M. Studnicka, Neutrophil extracellular trap (NET) formation characterises stable and exacerbated COPD and correlates with airflow limitation, Respir. Res. 16 (2015) 59. https://doi.org/10.1186/s12931-015-0221-7.
[30] B.G. Yipp, B. Petri, D. Salina, C.N. Jenne, B.N.V. Scott, L.D. Zbytnuik, K. Pittman, M. Asaduzzaman, K. Wu, H.C. Meijndert, S.E. Malawista, A. de Boisfleury Chevance, K. Zhang, J. Conly, P. Kubes, Infection-induced NETosis is a dynamic process involving

neutrophil multitasking in vivo, Nat. Med. 18 (2012) 1386–1393. https://doi.org/10.1038/nm.2847.
[31] B.G. Yipp, P. Kubes, NETosis: how vital is it?, Blood 122 (2013) 2784–2794. https://doi.org/10.1182/blood-2013-04-457671.
[32] J.-P. Pais de Barros, T. Gautier, W. Sali, C. Adrie, H. Choubley, E. Charron, C. Lalande, N. Le Guern, V. Deckert, M. Monchi, J.-P. Quenot, L. Lagrost, Quantitative lipopolysaccharide analysis using HPLC/MS/MS and its combination with the limulus amebocyte lysate assay, J. Lipid Res. 56 (2015) 1363–1369. https://doi.org/10.1194/jlr.D059725.
[33] A. Saraf, L. Larsson, H. Burge, D. Milton, Quantification of ergosterol and 3-hydroxy fatty acids in settled house dust by gas chromatography-mass spectrometry: comparison with fungal culture and determination of endotoxin by a Limulus amebocyte lysate assay, Appl. Environ. Microbiol. 63 (1997) 2554–2559. https://doi.org/10.1128/AEM.63.7.2554-2559.1997.
[34] M. Yang, H. Sang, A. Rahman, D. Wu, A.B. Malik, R.D. Ye, G alpha 16 couples chemoattractant receptors to NF-kappa B activation, J. Immunol. 166 (2001) 6885–6892. https://doi.org/10.4049/jimmunol.166.11.6885.
[35] M. Sundqvist, K. Christenson, A. Holdfeldt, M. Gabl, J. Mårtensson, L. Björkman, R. Dieckmann, C. Dahlgren, H. Forsman, Similarities and differences between the responses induced in human phagocytes through activation of the medium chain fatty acid receptor GPR84 and the short chain fatty acid receptor FFA2R, Biochimica et Biophysica Acta (BBA) - Molecular Cell Research 1865 (2018) 695–708. https://doi.org/10.1016/j.bbamcr.2018.02.008.
[36] G. Schett, M.F. Neurath, Resolution of chronic inflammatory disease: universal and tissue-specific concepts, Nat Commun 9 (2018) 3261. https://doi.org/10.1038/s41467-018-05800-6.
[37] C. Diskin, E.M. Pålsson-McDermott, Metabolic Modulation in Macrophage Effector Function, Front. Immunol. 9 (2018) 270. https://doi.org/10.3389/fimmu.2018.00270.
[38] L. Li, S.-Y. Shin, K.W. Lee, N.S. Han, Production of natural antimicrobial compound D-phenyllactic acid using Leuconostoc mesenteroides ATCC 8293 whole cells involving highly active D-lactate dehydrogenase, Letters in Applied Microbiology 59 (2014) 404–411. https://doi.org/10.1111/lam.12293.
[39] N. Rodríguez, J.M. Salgado, S. Cortés, J.M. Domínguez, Antimicrobial activity of d-3-phenyllactic acid produced by fed-batch process against Salmonella enterica, Food Control 25 (2012) 274–284. https://doi.org/10.1016/j.foodcont.2011.10.042.